ARTICLE   OPEN

Check for updates

Urban climate changes during the COVID-19 pandemic: integration of urban-building-energy model with social big data

Yuya Takane [1] [✉], Ko Nakajima [1] and Yukihiro Kikegawa [2]

The changes in human behaviour associated with the spread of COVID-19 infections have changed the urban environment. However, little is known about the extent to which they have changed the urban climate, especially in air temperature (T), anthropogenic heat emission (Q_F) and electricity consumption (EC). We quantitatively evaluated these effects using a unique method that integrates real-time human population data (social big data) with an urban climate model. The results showed that in an office district in the city centre of Tokyo, the biggest metropolis in the world, under a significantly reduced population, EC (CO_2 emissions) would be 30% and Q_F would be 33% of pre-COVID levels (without the stay-at-home advisories). This resulted in a T decrease of about 0.2 °C, representing about 20% of the past greenhouse gas-induced warming (about 1.0 °C) in Tokyo. This method can be benchmarked and then applied to worldwide. The results suggest that changes in human behaviour can represent an adaptation and decarbonising strategies to climate change in cities.

INTRODUCTION

The coronavirus SARS-CoV-2 (COVID-19) pandemic significantly changed human behaviour worldwide. In many major cities globally, the ensuing lockdowns greatly restricted human activity. In Japan, because the number of COVID-19 cases in Tokyo tended to increase clearly, a state of emergency was declared in April 2020, which reduced the daytime population in city office districts by more than 50% due to the promotion of teleworking at home (Supplementary Fig. 1a). After the declaration, the number of cases tended to decrease, so the state of emergency was lifted on 14 May (Supplementary Fig. 1a). This change in human behaviour during the state of emergency may continue to some extent after COVID-19, with the development of a 'new-normal' situation. Note that although the state of emergency in Japan was a self-restraint campaign, exactly not lockdown, the magnitude of human behaviour change was like that of lockdown.

Previous studies have reported how the lockdown and stay-at-home advisories have changed environments worldwide. For example, air quality has improved[1–5] and greenhouse gas (GHG) emissions have been reduced[6–10] due to lockdowns and stay-at-home advisories. According to Friedlingstein et al.[11], global CO_2 emissions from fossil fuels decreased by 5.4% due to the COVID-19 lockdown in 2020. However, the global temperature response due to COVID-19 restrictions will probably be small, and climate scientists are encouraged to look for regional climate signatures[3]. Now shifting the perspective from global to local, changes in CO_2 emissions have been directly observed in the urban areas where we live[7,9]. So, what was the impact on local temperature (urban heat islands) in cities where human activities strongly affect them? In this context, changes in the land-surface temperature (LST) due to lockdowns have also been reported[12,13]. In addition, the lockdown and stay-at-home advisories could have changed the urban climate in terms of urban near-surface air temperature (T), anthropogenic heat emissions (Q_F) and electricity consumption

(EC) because the urban climate is strongly affected by human behaviour[14]. However, only a few studies have attempted to estimate this effect based on the local climate[15–17]. The technical difficulty of detecting changes in urban T due to the pandemic is a limitation in such studies. From an observational perspective, it is not easy to clarify a pandemic signal (temperature change due to the stay-at-home advisories) in observed temperatures because the weather changes constantly due to natural variability. It is not possible to conclude that an urban temperature decrease/increase during lockdown was not just due to the natural variation in urban temperature.

Under such a limitation, a numerical simulation using urban parameterisations is a powerful tool, which could extract the pandemic signal. For example, urban parameterisation could estimate the impact of Q_F on urban T[18–26]. There is robust evidence and high agreement that urban parameterisations can be used to generally simulate radiation exchanges in a realistic way[27]. However, there is another limitation in the use of a numerical model due to its incomplete modelling of the relationship between urban climate and human behaviour. For example, a single-layer urban canopy model (UCM)[28] can handle the input of Q_F, which relates to human behaviour but does not directly express human behaviour (the avarage diurnal change in Q_F is input into the model). In this study, a coupled model, UCM with the building energy model (BEM) (hereafter, UCM–BEM)[16,29–31] was used to express human behaviour and simulate its effects on the urban climate (see the Methods section for details of how human behaviours were input into the model).

Using the UCM–BEM, a previous study attempted to estimate the impact of stay-at-home advisories due to COVID-19 on the urban climate[16]. The authors developed a simulation system that used real-time population and traffic data. More specifically, they estimated population and traffic changes due to COVID-19 and input these changes as the UCM–BEM parameters related to

[1]Environmental Management Research Institute, National Institute of Advanced Industrial Science and Technology (AIST), Tsukuba, Ibaraki, Japan. [2]School of Science and Engineering, Meisei University, Hino, Tokyo, Japan. [✉]email: takane.yuya@aist.go.jp

npj

human behaviour. This new modelling system showed that the COVID-19 stay-at-home advisories resulted in a Q_F of 76.3 W m^{-2} and a 0.13 °C air temperature reduction in urban areas in Osaka, the second-largest city in Japan. Although this work indicated the impact of COVID-19 on urban climate based on numerical simulations, there were some limitations. They did not consider the actual stay-at-home advisories period of COVID-19, and they used population change data on only one ideal office grid point in Osaka. To estimate the impact of COVID-19 on urban climate with more accuracy, it is necessary to conduct a simulation during the actual stay-at-home advisories period based on population change data for all of the grid points in a target area.

Estimations made using a numerical model are essential in areas related to global climate change, urban climate, sustainability, environment, human behaviour and urban planning. With cities predicted to be home to more than 66% of the global population by 2050[32], urban warming due to global warming and the urban heat island effect are critical issues[26,33–38]. Changes in human behaviour due to lockdowns and stay-at-home advisories could be an adaptation strategy to climate change in urban areas, but it remains unclear how effective those would be. In urban areas significantly affected by climate change[27], many 'hard-type' climate change adaptation strategies (traditional urban heat island mitigation techniques such as greening and cool roofs) have been proposed and evaluated[37,39,40]. A 'soft-type' strategy, such as a change in human behaviour, has yet to be assessed sufficiently, although some studies have already estimated weekday–weekend temperature differences[41–44]. The impact of changes in human behaviour on urban climate remains unknown. The COVID-19 pandemic could provide an opportunity to understand how human behaviour affects the urban climate based on scientific principles.

We estimated the impact of changes in human behaviour related to the COVID-19 pandemic on the urban climate in the world's biggest metropolitan area of Tokyo, which has a hot and humid climate during summer, using the UCM–BEM and real-time population and traffic data (social big data). Through this sophisticated estimation, we developed simple equations to estimate the impact on the whole of Japan and other countries with similar climates, building materials and human behaviour. The aim was to understand whether changes in human behaviour could be an adaptation strategy to climate change. To sum up, the novelties of our study are: (1) proposing a new method which is an integration of urban climate-building-energy model and social big data, (2) showing the COVID-19 impact on not only urban 'air' temperature (T), but also important urban climate-related variables: Q_F and EC (CO_2 emission), (3) proposing simple equations to estimate the COVID-19 impact on a more wide area and (4) providing basic information on whether human behaviour changes could be an adaptation strategy to climate change.

RESULTS AND DISCUSSION
Changes in human behaviour due to the COVID-19 pandemic
The population densities of the Tokyo Metropolitan Area (TMA) from 18 April to 14 May 2019 and 2020 (Fig. 1a, b) and its change ratio (2020/2019) (Fig. 1c) were plotted. Human activity was significantly changed by the pandemic. The population in the centre of Tokyo and its surrounding area decreased and increased, respectively (Fig. 1c). The traffic count differed from the population data (Fig. 1d, e, f). The traffic counts decreased in almost all areas of the TMA due to the stay-at-home advisories (Fig. 1f). These changes in population and traffic counts were used as human behavioural change parameters in the numerical model (see details in the Methods section).

Urban climate change in the Tokyo Metropolitan Area
After verification of the numerical model (see Supplementary Notes 2), we estimated the impact of COVID-19 induced human behavioural changes on the urban climate (Fig. 2).

We calculated the changes in EC (COVID minus No-COVID: ΔEC). The daytime (09:00–17:00 Japan Standard Time [JST]) EC in the centre of Tokyo (office area) decreased (Fig. 2a, b) due to the reduced population (Fig. 1c). For example, the number of people using the Tokyo railway station during the pandemic was only 39.4% of the pre-COVID level, and the EC during the pandemic was estimated to be 30.2% of the pre-COVID level (Table 1a). By contrast, the EC increased in residential areas (Fig. 2a, b) due to the increase in the daytime population (Fig. 1c). These ΔEC values were mainly due to changes in the baseload (EC for appliances that is not affected by changes in T) during the stay-at-home advisories period (April–May). This period was not the season when urban residents typically use space heating or cooling (Supplementary Fig. 1b). The EC was directly correlated with population change in terms of building use in commercial and business grids (office: hereafter, C), residential grids that predominantly consisted of fireproof apartments (Rm) and residential grids that were chiefly covered by wooden detached dwellings (Rd) (Fig. 2c). Based on the ΔEC, the changes in CO_2 emissions were estimated using the CO_2 emissions coefficient of 0.000445 (t-CO_2 kWh^{-1}) (https://www.env.go.jp/press/files/jp/115373.pdf). The estimation showed that daily total CO_2 emissions in the 23 wards of Tokyo decreased by 8.2% (8.06 t-CO_2 km^{-2} day^{-1}) due to the COVID-19 pandemic.

The ΔEC affected the daytime changes in Q_F (ΔQ_F). As with the ΔEC, the Q_F decreased due to the pandemic in the centre of Tokyo (Fig. 2d), with a reduction of about −1.3 GW in the total office grids (Fig. 2e), which is contributed by 88.2% from air-conditioning (AC) use ($\Delta Q_{F, AC}$) and by 11.8% from traffic ($\Delta Q_{F, TRA}$). The Q_F in the areas surrounding Rm was also reduced by a decrease in traffic (Fig. 1f). Figure 2f shows the relationship between the population change ratio and Q_F, and indicates that, as with the ΔEC, the ΔQ_F was also correlated with population change.

The ΔQ_F causes changes in the urban T (ΔT). Figure 2g shows the impact of the pandemic-induced human behavioural changes on daytime urban T and indicates that the temperature in the centre of Tokyo (C areas) decreased due to the pandemic. The temperature decrease reached −0.21 °C (Fig. 2h and Table 1a, Tokyo railway station). By contrast, there were no significant temperature changes in the surrounding areas (residential areas) (Fig. 2g, h). The relationship between the population change ratio and T change is shown in Fig. 2i, which indicates that T tended to decrease with population reduction in the office area (C). There was no clear relationship in the residential areas (Rd and Rm).

As in the daytime, the EC, Q_F and T were also impacted by the changes in human behaviour in the nighttime, but the impact was lower because nocturnal human behaviour during that time did not change significantly.

Application to the urban climate of all Japanese cities
Based on the detailed estimation using the model and the mobile spatial statistics (MSS) population data shown in the section 'Urban climate change in the Tokyo Metropolitan Area', we estimated the impact of the pandemic on the urban climate of all Japanese cities. There was a clear relationship between the population change ratio (ΔP) and, ΔEC, ΔQ_F, and ΔT (Fig. 2c, f, i), which could be used to estimate the impact of COVID-19 on the urban climate of other cities. We proposed the following
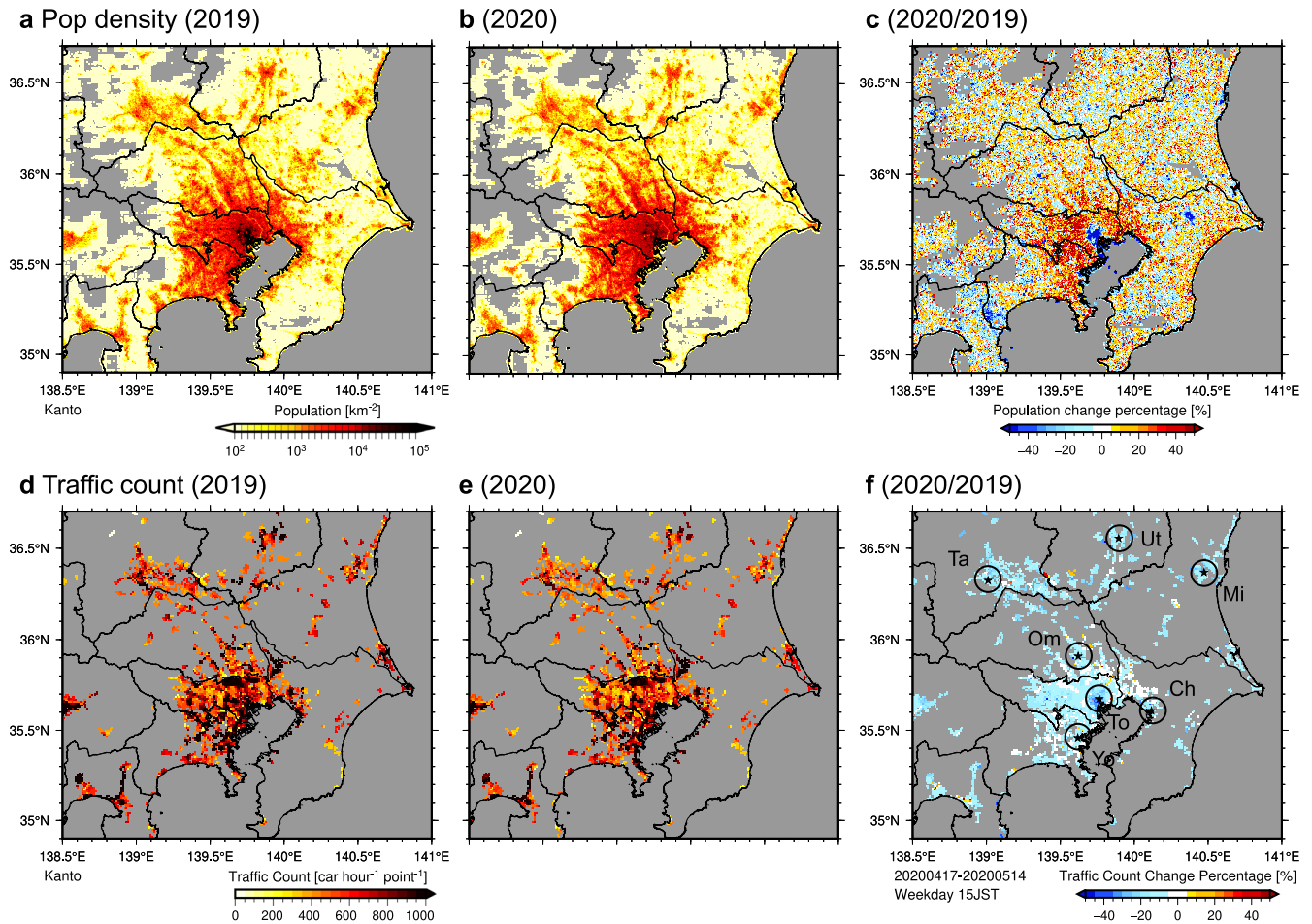
Fig. 1 Changes in human behaviour due to the COVID-19 pandemic. Horizontal variation in population densities (pop km^{-2}) for 15:00 Japan Standard Time (JST) **a** 18 April to 14 May 2019, **b** 2020, and **c** the 2020/2019 change ratio. Traffic counts for **d** 18 April to 14 May 2019, **e** 2020, and **f** the 2020/2019 change ratio and site locations of analysed point: To (Tokyo), Yo (Yokohama), Ch (Chiba), Om (Omiya), Mi (Mito), Ta (Takasaki), and Ut (Utsunomiya) on the Kanto Plain including the Tokyo Metropolitan Area (TMA).

equations:

$$\Delta EC_{i,j,t} = a\Delta P_{i,j,t} + b \tag{1}$$

$$\Delta Q_{F\,i,j,t} = c\Delta P_{i,j,t} + d \tag{2}$$

$$\Delta T_{i,j,t} = e\Delta P_{i,j,t} + f \tag{3}$$

where i and j are the grid numbers in the zonal and meridional direction, t is hours, and a (c, e) and b (d, f) are the slope and intercept, respectively (Supplementary Table 1). These relationships were used for the simple estimation of the impact of COVID-19 on the urban climate of all Japanese cities. For example, it was possible to estimate the impact of changes in human behaviour on the EC of all Japanese cities using just a linear Eq. (1), actual population change data and land-use data (urban categories: C, Rd, and Rm) (Supplementary Fig. 3b) for all Japan cities. Similarly, the impact on Q_F and T could also be estimated.

Figure 3c shows the estimated ΔEC using Eq. (1) for TMA. The horizontal distribution of ΔEC (Fig. 2a) simulated by the sophisticated model was reproduced using equation (1). Based on the above, Fig. 3 and Table 1b indicate that EC decreased due to the pandemic in all major city centres in Japan. Similarly, it was possible to estimate the impact on CO_2 emissions and Q_F, with similar results to those obtained for EC (Table 1b). These simple equations we developed were used to estimate the impact on cities in Japan and other countries with similar climates, building materials, lifestyles and AC usage.

Comparison with observations and previous estimations

The results of this study and previous studies are summarised in Table 2. Note that we do not compare our result with previous works focused on the COVID-19 impact on LST as it is impossible to directly compare our estimated urban 'air' temperature and LST. A maximum temperature decrease of about −0.2 °C was estimated for Tokyo's office district due to the pandemic. This temperature decrease was consistent with the reported temperature decrease of about −0.1 °C in central Osaka, which was previously estimated using the same method[16]. More importantly, the calculated results were consistent with the temperature decrease in central Tokyo and cities in China previously estimated from observations and a statistical analysis (−0.40 ± 0.21 °C[15] and −0.42 ± 0.26 °C[17]), which was an entirely different approach from the present study. The consistency between results suggests that ΔT could be estimated realistically.

As described in the introduction, only a few studies have evaluated ΔT induced by the COVID-19 pandemic, and comparisons with the results of previous studies are therefore limited. Instead, our results are compared to those of studies that have assessed the effects of introducing urban planning scenarios on T. Specifically, Adachi et al.[45] and Kusaka et al.[46] estimated the impact of a dispersed city, i.e., an urban planning scenario in which offices and other functions are distributed around the city centre, rather than being concentrated in the city centre. Because commuting to the city centre was significantly reduced during the state of emergency period (Fig. 1), the voluntary restraint on going
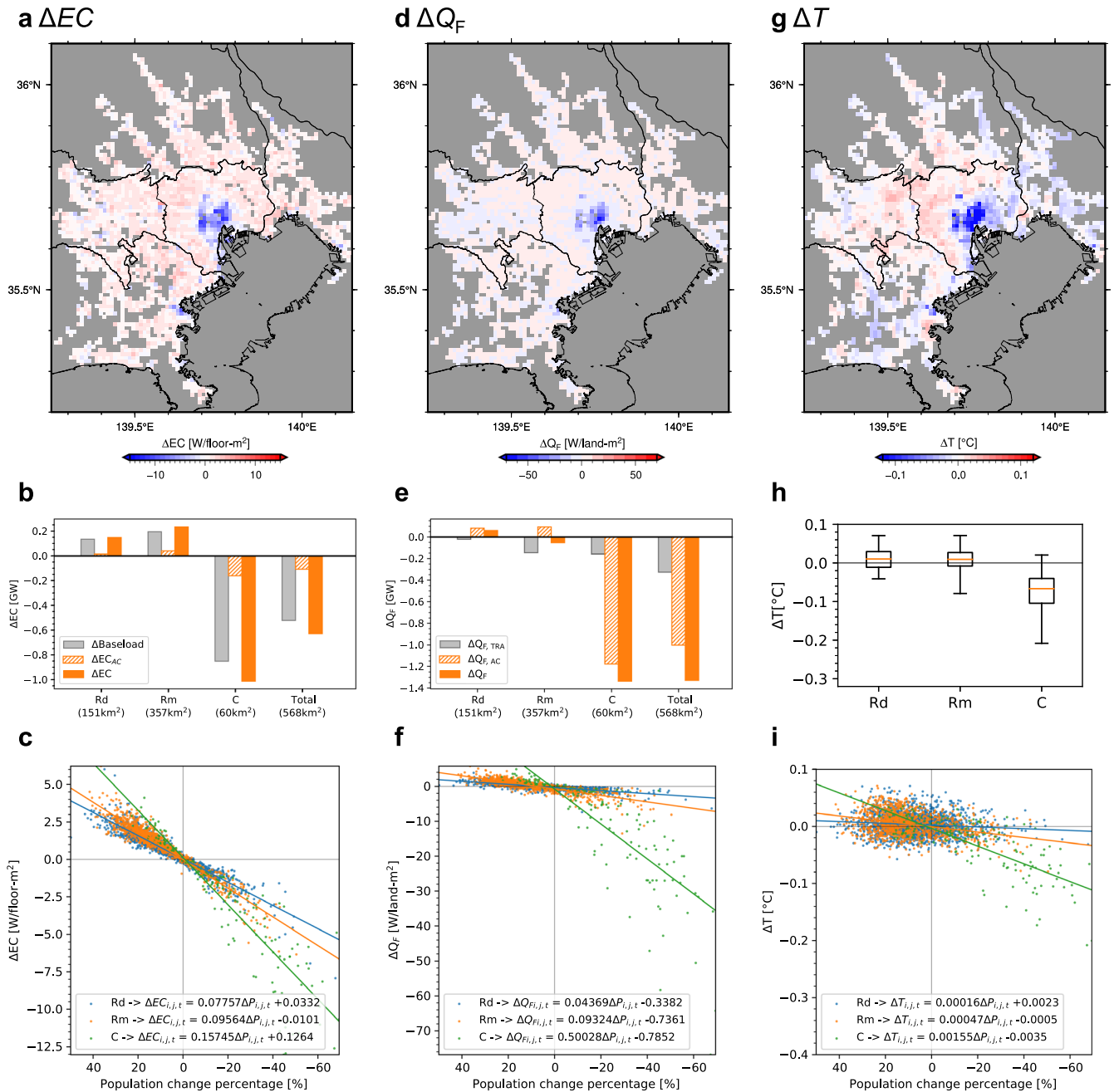
Fig. 2 Impact of COVID-19 on urban climate. Horizontal variation in the impact of COVID-19 on **a** energy consumption (*EC*) (ΔEC), **d** anthropogenic heat (Q_F) (ΔQ_F) and **g** near-surface air temperature (*T*) (ΔT) as a daytime average for the period of 18 April to 14 May 2020. Bar charts and box plots of **b** ΔEC, **e** ΔQ_F and **h** ΔT for each urban category and the total for the 23 wards of Tokyo (bold black line in **a**, **d**, and **g**). The relationship between population changes and **c** ΔEC, **f** ΔQ_F and **i** ΔT for each urban category.

out due to the pandemic could cause a similar situation in terms of commuter behaviour compared with that in a dispersed city. Therefore, we compared our results of a temperature decrease of about −0.2 °C, with those of Adachi et al.[45] and Kusaka et al.[46]. The dispersed city scenario was estimated to induce negative ΔT reaching −0.2–0.3 °C in the city centre (Table 2). Our estimate is almost the same. Thus, the stay-at-home advisories can be viewed as a kind of social experiment similar to the introduction of dispersed cities. To create a dispersed city, offices need to be moved from the city centre to the suburbs, which costs money. Promoting remote work would therefore be more cost-effective than developing a dispersed city.

Furthermore, the temperature difference between weekdays and holidays was compared to the *T* drop of −0.2 °C recorded in this study. Temperatures are lower in office areas in central Tokyo on weekends than on weekdays because fewer working people on weekends there[41–43,47,48]. The stay-at-home advisories could induce a situation resembling a holiday almost every day. Therefore, comparing the temperature difference between weekdays and holidays is essential. In estimates made in previous studies, the temperature on holidays was −0.1–0.6 °C lower than on weekdays (Table 2). Our values are consistent, which implies that the estimated impacts of this study are reasonable. The numerical model used in this study reproduced the difference between observed weekday and holiday temperatures well and

Table 1. Summary of the relationships between the changes in population and urban climate.

a

	Tokyo Sta (To)	Yokohama Sta (Yo)	Chiba Sta (Ch)	Omiya Sta (Om)	Mito Sta (Mi)	Takasaki Sta (Ta)	Utsunomiya Sta (Us)
Population (2020/2019×100, %)	39.4	50.0	66.8	79.3	86.7	80.6	83.6
EC and CO_2 (COVID/no-COVID×100, %)	30.2	37.8	56.0	73.1	72.0	67.7	75.0
Q_F (COVID/no-COVID×100, %)	32.8	62.4	65.1	82.1	79.8	77.1	83.6
ΔT (COVID – no-COVID, °C)	−0.21	−0.08	−0.08	−0.02	0.03	−0.02	−0.01

b

	Sapporo (Hokkaido)	Sendai (Miyagi)	Tokyo (Tokyo)	Nagoya (Aichi)	Kyoto (Kyoto)	Osaka (Osaka)	Kobe (Hyogo)	Fukuoka (Fukuoka)
Population (2020/2019×100, %)	56.6	59.1	39.4	40.1	45.4	38.4	55.3	49.7
ΔEC (W floor m^{-2})	−6.7	−6.3	−12.3	−9.3	−4.2	−9.6	−6.9	−7.8
ΔQ_F (W m^{-2})	−22.5	−21.2	−75.6	−30.8	−2.7	−31.6	−23.2	−25.9
ΔT (°C)	−0.07	−0.07	−0.21	−0.10	−0.01	−0.10	−0.07	−0.08

At seven railway stations on the Kanto Plain, including **a** the Tokyo Metropolitan Area (TMA) (see Fig. 1f) and for **b** nine major cities in Japan (see Fig. 3).

was used for calculations in cities[49], and it was therefore reasonable to make the above comparison. Finally, the Chinese New Year (CNY) influenced the impact of changes in human behaviour on T. The impact was about −0.6 °C[44,50–52], and therefore the impact of the stay-at-home advisories in Japan tended to be smaller than that of CNY, although the order of magnitude was comparable.

In terms of CO_2 emissions, we estimated that emissions during COVID were about 7% smaller than during the No-COVID period in the residential area of Tokyo, which qualitatively agrees with the changes in the observed CO_2 flux in the same area reported by Sugawara et al.[9].

Could changes in human behaviour be a climate change adaptation in urban areas?

The section 'Urban climate change in the Tokyo Metropolitan Area' shows the urban climate change due to the pandemic in the spring season when AC is rarely used. In the future, it is likely that AC usage will increase as urban temperatures increase leading to high levels of heat stress[26,38,53–55]. To assess the potential for climate change adaptation in cities, it was necessary to estimate how the urban climate changed due to the pandemic during summer when AC is often used. Although the state of emergency was lifted by 25 May, social activity was suppressed in summer due to the re-spread of infection. Therefore, we estimated the impact of COVID-19 stay-at-home advisories on the summer urban climate and compared the effect with widely adopted climate change adaptation strategies (e.g., greening and cool roofs). In the summertime simulation, we conducted ran from 09:00 JST on 27 July to 09:00 JST on 1 September 2020 and used the same as the population change ratio (ΔP^{COVID}) and the traffic count ratio (Δtra) (see Methods) as used in April–May simulation shown in the section 'Results and discussion'.

Supplementary Fig. 2 shows the impact of the pandemic on urban climate in terms of EC (ΔEC), Q_F (ΔQ_F) and T (ΔT) during the summer period. The daytime EC in the centre of Tokyo decreased (Supplementary Fig. 2a) due to the population reduction (Fig. 1c) and limited AC use. By contrast, there was a large EC increase in the residential areas (Supplementary Fig. 2a, b) due to the daytime population increase (Fig. 1c) and high levels of AC use. This trend was supported by observations using a smart meter in residential houses in Japan (not shown). These ΔEC values were caused by changes in the baseload and AC use (Supplementary Fig. 2b). The EC was directly correlated with the changes in the occupancy of buildings (Supplementary Fig. 2c). The estimation showed that the daily total CO_2 emissions in the 23 wards of Tokyo decreased by 7.9% (11.07 t-CO_2 km^{-2} day^{-1}) due to the COVID-19 pandemic.

The Q_F in summer decreased much more than in spring due to the pandemic in the centre of Tokyo (Supplementary Fig. 2d versus Fig. 2d), with the amount being about −3.1 GW in the office grids (Supplementary Fig. 2e). By contrast, the Q_F in the Rm areas increased due to AC use, although the traffic count decreased (Supplementary Fig. 2e and Fig. 1f). Supplementary Fig. 2f shows the relationship between the population change ratio and ΔQ_F, which indicated that the ΔQ_F was much more strongly correlated with population change than the temperature in spring (Supplementary Fig. 2f versus Fig. 2f).

The ΔT in the centre of Tokyo (office area) was −0.30 °C, which was a more significant impact than in spring (Supplementary Fig. 2h versus Fig. 2h) and was equivalent to 30% of the past GHG-induced warming in Tokyo: the warming in Tokyo is largely influenced by urbanisation, and the contribution of GHGs is likely to be 1 °C or so[56]. In contrast to office areas, the temperature increased in the surrounding areas (residential areas) (Supplementary Fig. 2g, h). This increase was also much more significant than in spring (Supplementary Fig. 2h versus Fig. 2h). The relationship between the population change and
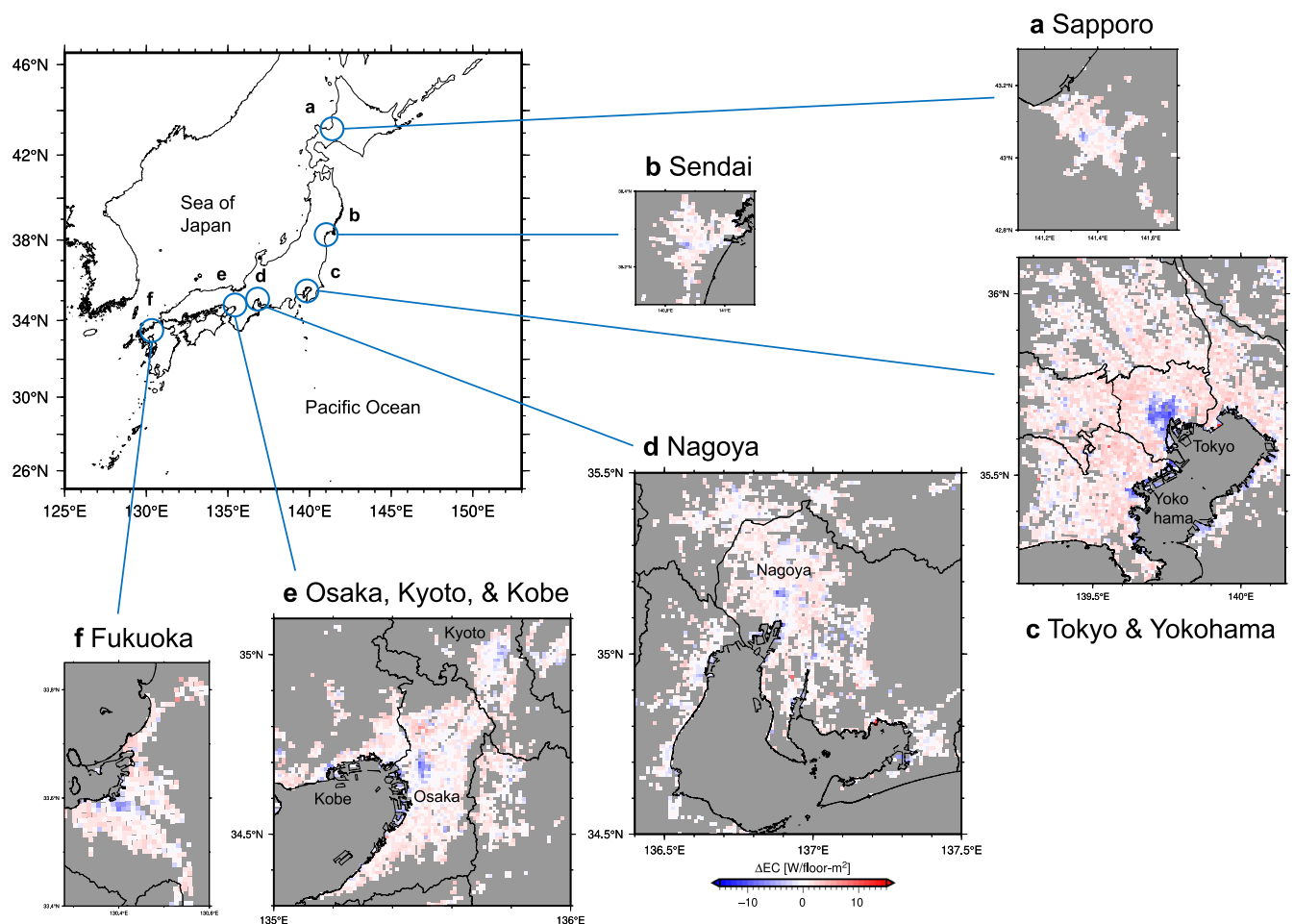
Fig. 3 Change in electricity consumption (ΔEC) for six major metropolises in Japan. a Sapporo (Hokkaido), **b** Sendai (Miyagi), **c** Tokyo (Tokyo) and Yokohama (Kanagawa), **d** Nagoya (Aichi), **e** Osaka (Osaka), Kyoto (Kyoto) and Kobe (Hyogo), and **f** Fukuoka (Fukuoka).

temperature change is shown in Supplementary Fig. 2i, which suggests that temperature tended to decrease/increase with population changes in office area C and residential areas (Rd and Rm). respectively.

The magnitude of the temperature change (ΔT) may increase under future climate change because many urban residents will begin to use AC, and the thermal heat load will be increased by the increase in outdoor temperature[26,38,57]. The summertime ΔT presented above is comparable/similar to that attained by adopting the well-known urban heat island countermeasure techniques[37,39] (e.g., cool roofs and greening[58]). An advantage of the change in human behaviour induced by the pandemic as an adaptation strategy is that there are no/small introduction and running costs. In addition, such changes in human behaviour could reduce exposure to high-heat stress in the outdoor environment. Future studies should estimate the combined effects of this change in human behaviour (a 'soft-type' strategy) and other well-known adaptation strategies, such as greening and cool roofs (a 'hard-type' strategy)[37,39].

METHODS

Human behaviour and traffic data (social big data)
We used MSS data regarding the stay-at-home advisories (18 April to 14 May 2020) and the same dates in 2019 (18 April to 14 May 2019) provided by NTT Docomo, Inc. The MSS data provided population statistics based on the location of 78 million users of NTT Docomo's mobile terminals in the

whole Japan. The MSS data are created from this information[16]. First, the number of mobile terminals in each base station area was aggregated. Second, the total number of mobile terminals was extrapolated based on the adoption rates of NTT Docomo mobile terminals. Finally, the estimated population was re-aggregated into each grid section. More details of the MSS estimation method are provided by Terada et al.[59]. The temporal and spatial resolutions of MSS data were 1 h and 500 m, respectively. Previously, MSS data have been used to estimate human activity in urban climates[16]. Other population data such as location trends were provided by KDDI, Inc. and the Japan Travel Guide of NTT Advertising, Inc.; however, their sample numbers were relatively small[60]. Thus, MSS provides data that can be used to examine real-time changes in specific populations.

The level of traffic congestion is related to the Q_F derived from automobiles ($Q_{F, TRA}$). To estimate the changes in traffic volumes during the stay-at-home advisories, we used traffic counts for public roads at 5-min intervals for 8060 sites in TMA in April–May 2019 and 2020. These data were provided by the Japan Road Traffic Information Center and were distributed by the Japan Traffic Management Technology Association.

Model
The study used the Advanced Research WRF (ARW) ver. 3.7.1[61] and the online coupling of WRF and CM-BEM[29] (hereafter, WRF–CM–BEM[16,62]). Supplementary Fig. 3 shows the model domain that covered the area of Japan, including TMA, which was the focus of our study. The d01, d02 and d03 domains consisted of 89, 110 and 250 grid points, respectively, in the x and y directions. We set the horizontal grid spacing to 25, 5 and 1 km in the domains d01, d02 and d03, respectively. The model top was 50 hPa, with 34 vertical sigma levels. In this simulation, the initial and boundary

Table 2. Summary of the results of previous studies and this study.

Target	Signal	City	Method	Ref.
Stay-at-home/lockdown	−0.2 °C (daytime)	Tokyo, Japan	Numerical experiments	This study
	About −0.1 °C (daytime)	Osaka, Japan	Numerical experiments	Nakajima et al.[16]
	−0.40 ± 0.21 °C (daytime) No signal	Tokyo, Japan Osaka, Japan	Observation and statistical analysis	Fujibe[15]
	−0.42 ± 0.26 °C (daytime)	Cities in China	Observation and statistical analysis	Liu et al.[17]
Dispersed city scenario	About −0.3 °C (nighttime)	Tokyo, Japan	Numerical experiments	Adachi et al.[45]
	−0.2~0.25 °C (daytime)	Tokyo, Japan	Numerical experiments	Kusaka et al.[46]
Weekday–weekend differences	−0.2~0.25 °C (daytime) −0.10~0.20 °C (daytime) (weekends < weekdays)	Tokyo, Japan Osaka, Japan	Observation and statistical analysis	Fujibe[41,42]
	−0.13~0.37 °C (mean)	12 cities in Germany	Observation and statistical analysis	Bäumer and Vogel[47]
	−0.2~0.6 °C (daytime) (weekends < weekdays)	Osaka, Japan	Observation and statistical analysis	Ohashi et al.[43]
	−0.1~0.2 °C (09 LT) −0.1~0.4 °C (09 LT)	Melbourne, AU Sydney, AU	Observation and statistical analysis	Earl et al.[48]
Mass human movements (Chinese New Year holiday)	−0.65 °C (daily mean)	Harbin, China	Observation and statistical analysis	Wu et al.[50]
	−0.64 °C (daily mean)	Beijing, China	Observation and statistical analysis	Zhang et al.[51]
	About −0.6 °C (daily mean)	Beijing, China	Observation and statistical analysis	Zhang and Wu[52]
	−0.3~0.6 °C	Beijing, China	Observation and statistical analysis	Dou and Miao[44]

conditions were derived from the National Centers for Environmental Prediction–National Center for Atmospheric Research reanalysis data[63].

The following schemes were used in the simulation: the updated Rapid Radiation Transfer Model longwave scheme[64], the Goddard shortwave scheme[65,66], the Thompson microphysics scheme[67], the Mellor–Yamada–Janjic atmospheric boundary-layer scheme[68–70], the Noah land surface model[71], and the CM-BEM[29,62] for the TMA and a single-layer urban canopy[28,72,73] in some urban grids around the city centre.

As in Takane et al.[23] and Nakajima et al.[16], building footprint (polygon) data from a geographical information system in the TMA were used to identify urban canopy geometry were being used. The building use and total floor area for each building in the TMA were recorded. Land use and land cover (LULC) data and topographic datasets of the Geospatial Information Authority of Japan (GIAJ) were used in this study. In addition to the GIAJ LULC data, the ArcGIS Geo Suite provided by ESRI-Japan Co., Ltd. (esrij.com/products/data-content-geosuite-shosai/) and a land-use survey performed in the 2016 fiscal year by the Bureau of Urban Development of the Tokyo Metropolitan Government were used for classification. The urban grids were classified into three categories (C, Rm and Rd) based on the dominant building type, as shown in Supplementary Fig. 3b. In the study, when we analysed each category, we only used the grids for those categories within the TMA.

The model used in this study required the identification of parameters for the detailed building energy calculations. For the geometric parameters of urban canopies, the mean building width, mean distance between buildings, and distribution of building height had to be set in every urban grid. These settings were derived from the same building footprint data and were summarised in Supplementary Table 2. For the building energy simulation, the diurnal variation in the number of occupants, and AC systems were based on the values in the literature for the three-urban categories (Supplementary Fig. 3). More details of the parameters are provided in previous studies[23,26,38,62,74–76]. Note that we set the EC for appliances (baseload EC) in every urban grid based on actual EC data presented by Nakajima et al.[16,77].

As with Kikegawa et al.[62] and Nakajima et al.[16,77], the hourly total consumption of motor fuels in each grid, with a temporal resolution of 1 h, was estimated using traffic census data[78] and fuel economy data[79]. The combustion heat was obtained as the $Q_{F, TRA}$.

We also used the Automated Meteorological Data Acquisition System (AMeDAS) data for TMA provided by the Japan Meteorological Agency (JMA) as meteorological data.

The simulation was carried out from 09:00 JST (00:00 UTC = 09:00 JST) on 12 April to 09:00 JST on 17 May 2020 (Supplementary Fig. 1b). The first 5 days were discarded and considered the model spin-up. In this study, we referred to this simulation as the No-COVID case. For comparison with the April–May simulation, we conducted a summertime simulation, which ran from 09:00 JST on 27 July to 09:00 JST on 1 September 2020 (see the section 'Model', Supplementary Fig. 1c).

In addition to the No-COVID case, another case (COVID) was also conducted to estimate the impact of COVID-19 stay-at-home advisories in the city. Because the population and traffic count during the COVID case differed from those of usual days (Fig. 1), we modified the human behaviour parameters (the number of occupants, EC for appliances and AC operation schedule) and $Q_{F,TRA}$ (Fig. 4b) using the population change ratio of the stay-at-home advisories period to the usual days (ΔP^{COVID}) (Fig. 4a) and the traffic count ratio of the stay-at-home advisories period to the usual days (Δtra) (Fig. 4c). The ΔP^{COVID} and Δtra values are plotted in Fig. 1c, f, respectively. The modified human behavioural parameters (X^{COVID}) of each grid were calculated for the working hours (08:00–22:00 JST) on the stay-at-home advisories period as follows (Fig. 4b):

$$X^{COVID}_{i,j,t} = X^{No-COVID}_{i,j,t} \times \Delta P^{COVID}_{i,j,t} \ for \ t = 8, 9, ..., 21, 22 \ JST \tag{4}$$

where i and j are the grid numbers in the zonal and meridional directions, respectively, t is hours and $X^{No-COVID}$ is the human behaviour parameter in the No-COVID case (see Fig. 4b).

Similarly to the aforementioned parameters, the diurnal variation in $Q_{F, TRA}$ in the stay-at-home advisories period ($Q_{F, TRA}^{COVID}$) was calculated as follows:

$$Q^{COVID}_{F,TRA \ i,j,t} = Q^{No-COVID}_{F,TRA \ i,j,t} \times \Delta t_{TRA i,j,t} \ for \ t = 0, 1, ..., 22, 23 \ JST \tag{5}$$

where $Q_{F, TRA}^{No-COVID}$ is $Q_{F, TRA}$ in No-COVID.

Any other setting of COVID is the same as No-COVID except for the above human behaviour parameters.

DATA AVAILABILITY

The downscaling data produced by the WRF were deposited in local storage at AIST. These are available from the corresponding author upon reasonable request. The source code of the WRF and forcing data that support the findings of this study are available from http://www2.mmm.ucar.edu/wrf/users/ and https://rda.ucar.edu/, respectively. The observational data used in this study are available from the JMA website: https://www.jma.go.jp/jma/index.html. The population and traffic count data are available from https://mobaku.jp/ and https://www.jartic.or.jp/service/opendata/, respectively.
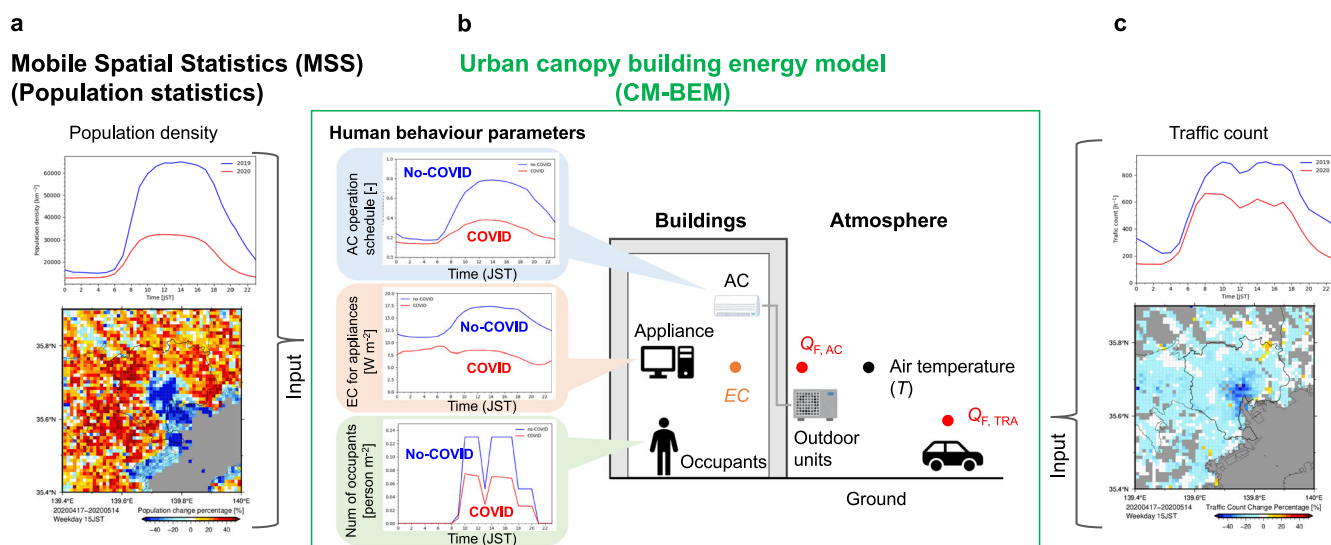
Fig. 4 Schematic view of an integration of urban-building-energy-model with social big data. a MSS, **b** UCM-BEM, and **c** traffic count data. The red and blue lines indicate human behaviours in the COVID and No-COVID cases, respectively.

CODE AVAILABILITY
The source codes of the WRF that support the findings of this study are available from http://www2.mmm.ucar.edu/wrf/users/.

REFERENCES
1. Zhu, Y., Xie, J., Huang, F. & Cao, L. Association between short-term exposure to air pollution and COVID-19 infection: evidence from China. *Sci. Total Environ.* **727**, 138704 (2020).
2. Bauwens, M. et al. Impact of Coronavirus outbreak on NO_2 pollution assessed using TROPOMI and OMI observations. *Geophys. Res. Lett.* **47**, e2020GL087978 (2020).
3. Forster, P. M. et al. Current and future global climate impacts resulting from COVID-19. *Nat. Clim. Chang* **10**, 913–919 (2020).
4. Samani, P., García-Velásquez, C., Fleury, P. & der Meer, Y. The impact of the COVID-19 outbreak on climate change and air quality: four country case studies. *Glob. Sustainability* **4**, 1–15 (2021).
5. Evangeliou, N. et al. Changes in black carbon emissions over Europe due to COVID-19 lockdowns. *Atmos. Chem. Phys.* **21**, 2675–2692 (2021).
6. Le Quéré, C. et al. Temporary reduction in daily global CO_2 emissions during the COVID-19 forced confinement. *Nat. Clim. Chang* **10**, 647–653 (2020).
7. Turner, A. J. et al. Observed impacts of COVID-19 on urban CO_2 emissions. *Geophys. Res. Lett.* **47**, e2020GL090037 (2020).
8. Jones, C. D. et al. The climate response to emissions reductions due to COVID-19: initial results from CovidMIP. *Geophys. Res. Lett.* **48**, e2020GL091883 (2021).
9. Sugawara, H. et al. Anthropogenic CO_2 emissions changes in an urban area of Tokyo, Japan, due to the COVID-19 pandemic: a case study during the state of emergency in April–May 2020. *Geophys. Res. Lett.* **48**, e2021GL092600 (2021).
10. Bertram, C. et al. COVID-19-induced low power demand and market forces starkly reduce CO_2 emissions. *Nat. Clim. Chang* **11**, 193–196 (2021).
11. Friedlingstein, P. et al. Global Carbon Budget 2021. *Earth Syst. Sci. Data Discuss* **14**, 1917–2005. https://doi.org/10.5194/essd-2021-386] (2022).
12. Parida, B. R. et al. Impact of COVID-19 induced lockdown on land surface temperature, aerosol, and urban heat in Europe and North America. *Sustain. Cities Soc.* **75**, 103336 (2021).
13. Chakraborty, T. C., Sarangi, C. & Lee, X. Reduction in human activity can enhance the urban heat island: insights from the COVID-19 lockdown. *Environ. Res. Lett.* **16**, 054060 (2021).
14. Oke, T. R., Mills, G., Christen, A. & Voogt, J. A. *Urban Climates*. (Cambridge Univ. Press, Cambridge, 2017).
15. Fujibe, F. Temperature anomaly in the Tokyo Metropolitan Area during the COVID-19 (coronavirus) self-restraint period. *Sci. Online Lett. Atmosphere* **16**, 175–179 (2020).
16. Nakajima, K., Takane, Y., Kikegawa, Y., Furuta, Y. & Takamatsu, H. Human behaviour change and its impact on urban climate: Restrictions with the G20 Osaka Summit and COVID-19 outbreak. *Urban Clim.* **35**, 100728 (2021).
17. Liu, Z. et al. Urban heat islands significantly reduced by COVID-19 lockdown. *Geophys. Res. Lett.* **49**, e2021GL096842 (2022).
18. Kimura, F. & Takahashi, S. The effects of land-use and anthropogenic heating on the surface temperature in the Tokyo Metropolitan area: a numerical experiment. *Atmos. Environ.* **25**, 155–164 (1991).
19. Ichinose, T., Shimodozono, K. & Hanaki, K. Impact of anthropogenic heat on urban climate in Tokyo. *Atmos. Environ.* **33**, 3897–3909 (1999).
20. Ohashi, Y. et al. Influence of air-conditioning waaste heat on air temperature in Tokyo during summer: numerical experiments using an urban canopy model coupled with a building energy model. *J. Appl Meteorol. Climatol.* **46**, 66–81 (2007).
21. De Munck, C. et al. How much can air conditioning increase air temperatures for a city like Paris, France? *Int J. Climatol.* **33**, 210–227 (2013).
22. Salamanca, F., Georgescu, M., Mahalov, A., Moustaoui, M. & Wang, M. Anthropogenic heating of the urban environment due to air conditioning. *J. Geophys. Res. Atmos.* **119**, 5949–5965 (2014).
23. Takane, Y. et al. A climatological validation of urban air temperature and electricity demand simulated by a regional climate model coupled with an urban canopy model and a building energy model in an Asian megacity. *Int J. Climatol.* **37**, 1035–1052 (2017).
24. Wang, Y., Li, Y., Sabatino, S., Di Martilli, A. & Chan, P. W. Effects of anthropogenic heat due to air-conditioning systems on an extreme high temperature event in Hong Kong. *Environ. Res. Lett.* **13**, 034015 (2018).
25. Xu, X. et al. Using WRF-Urban to assess summertime air conditioning electric loads and their impacts on urban weather in Beijing. *J. Geophys. Res. Atmos.* **123**, 2475–2490 (2018).
26. Takane, Y., Kikegawa, Y., Hara, M. & Grimmond, C. S. B. Urban warming and future air-conditioning use in an Asian megacity: importance of positive feedback. *NPJ Clim. Atmos. Sci.* **2**, 39 (2019).
27. IPCC. *AR6 Climate Change 2021: The Physical Science Basis* (2021).
28. Kusaka, H., Kondo, H., Kikegawa, Y. & Kimura, F. A simple single-layer urban canopy model for atmospheric models: Comparison with multi-layer and slab models. *Bound. Layer. Meteorol.* **101**, 329–358 (2001).
29. Kikegawa, Y., Genchi, Y., Yoshikado, H. & Kondo, H. Development of a numerical simulation system toward comprehensive assessments of urban warming countermeasures including their impacts upon the urban buildings' energy-demands. *Appl. Energy* **76**, 449–466 (2003).
30. Salamanca, F., Krpo, A., Martilli, A. & Clappier, A. A new building energy model coupled with an urban canopy parameterization for urban climate simulations—part I. formulation, verification, and sensitivity analysis of the model. *Theor. Appl. Climatol.* **99**, 331 (2010).
31. Salamanca, F. & Martilli, A. A new Building Energy Model coupled with an Urban Canopy Parameterization for urban climate simulations—part II. Validation with one dimension off-line simulations. *Theor. Appl. Climatol.* **99**, 345 (2010).

32. United Nations, Department of Economic and Social Affairs. *World Urbanization Prospects: The 2014 Revision (ST/ESA/SER.A/366)* (2015).

33. Oleson, K. Contrasts between urban and rural climate in CCSM4 CMIP5 climate change scenarios. *J. Clim.* **25**, 1390–1412 (2012).

34. Kusaka, H., Hara, M. & Takane, Y. Urban climate projection by the WRF model at 3–km grid increment: dynamical downscaling and predicting heat stress in the 2070's August for Tokyo, Osaka, and Nagoya. *J. Meteorol. Soc. Jpn.* **90B**, 47–64 (2012).

35. Georgescu, M., Moustaoui, M., Mahalov, A. & Dudhia, J. Summer-time climate impacts of projected megapolitan expansion in Arizona. *Nat. Clim. Chang* **3**, 37–41 (2013).

36. Varquez, A. C. G. & Kanda, M. Global urban climatology: a meta-analysis of air temperature trends (1960-2009). *NPJ Clim. Atmos. Sci.* **1**, 32 (2018).

37. Krayenhoff, E. S., Moustaoui, M., Broadbent, A. M., Gupta, V. & Georgescu, M. Diurnal interaction between urban expansion, climate change and adaptation in US cities. *Nat. Clim. Chang* **8**, 1097–1103 (2018).

38. Takane, Y., Ohashi, Y., Grimmond, C. S. B., Hara, M. & Kikegawa, Y. Asian megacity heat stress under future climate scenarios: impact of air-conditioning feedback. *Environ. Res. Commun.* **2**, 015004 (2021).

39. Georgescu, M., Morefield, P. E., Bierwagen, B. G. & Weaver, C. P. Urban adaptation can roll back warming of emerging megapolitan regions. *Proc. Natl Acad. Sci. USA.* **111**, 2909–2914 (2014).

40. Wong, N. H., Tan, C. L., Kolokotsa, D. D. & Takebayashi, H. Greenery as a mitigation and adaptation strategy to urban heat. *Nat. Rev. Earth Environ.* **2**, 166–181 (2021).

41. Fujibe, F. Weekday-weekend differences of urban climates Part 1: temporal variation of air temperature. *J. Meteorol. Soc. Jpn.* **65**, 923–929 (1987).

42. Fujibe, F. Day-of-the-week variations of urban temperature and their long-term trends in Japan. *Theor. Appl. Climatol.* **104**, 393–401 (2010).

43. Ohashi, Y. et al. Impact of seasonal variations in weekday electricity use on urban air temperature observed in Osaka, Japan. *Q J. R. Meteorol. Soc.* **142**, 971–982 (2016).

44. Dou, J. & Miao, S. Impact of mass human migration during Chinese New Year on Beijing urban heat island. *Int J. Climatol.* **37**, 4199–4210 (2017).

45. Adachi, S. et al. Moderation of summertime heat island phenomena via modification of the urban form in the Tokyo Metropolitan Area. *J. Appl Meteorol. Climatol.* **53**, 1886–1900 (2014).

46. Kusaka, H., Suzuki-Parker, A., Aoyagi, T., Adachi, S. A. & Yamagata, Y. Assessment of RCM and urban scenarios uncertainties in the climate projections for August in the 2050s in Tokyo. *Clim. Change* **137**, 427–438 (2016).

47. Bäumer, D. & Vogel, B. An unexpected pattern of distinct weekly periodicities in climatological variables in Germany. *Geophys. Res. Lett.* **34**, L03819 (2007).

48. Earl, N., Simmonds, I. & Tappe, N. Weekly cycles in peak time temperatures and urban heat island intensity. *Environ. Res. Lett.* **11**, 074003 (2016).

49. Kikegawa, Y., Nakajima, K., Takane, Y., Ohashi, Y. & Ihara, T. A quantification of classic but unquantified positive feedback effects in the urban-building-energy-climate system. *Appl. Energy* **307**, 118227 (2022).

50. Wu, L.-Y., Zhang, J.-Y. & Shi, C.-X. Mass human migration and the urban heat iisland during the Chinese new year holiday: a case study in Harbin city, Northeast China. *Atmos. Ocean. Sci. Lett.* **8**, 63–66 (2015).

51. Zhang, J., Wu, L., Yuan, F., Dou, J. & Miao, S. Mass human migration and Beijing's urban heat island during the Chinese New Year holiday. *Sci. Bull.* **60**, 1038–1041 (2015).

52. Zhang, J. & Wu, L. Influence of human population movements on urban climate of Beijing during the Chinese New Year holiday. *Sci. Rep.* **7**, 45813 (2017).

53. Takane, Y. & Kusaka, H. Formation mechanisms of the extreme high surface air temperature of 40.9°C observed in the Tokyo metropolitan area: considerations of dynamic foehn and foehnlike wind. *J. Appl Meteorol. Climatol.* **50**, 1827–1841 (2011).

54. Takane, Y., Kusaka, H. & Kondo, H. Climatological study on mesoscale extreme high temperature events in inland of the Tokyo metropolitan area, Japan, during the past 22 years. *Int J. Climatol.* **34**, 3926–3938 (2014).

55. Takane, Y., Kusaka, H. & Kondo, H. Investigation of a recent extreme high-temperature event in the Tokyo metropolitan area using numerical simulations: the potential role of a 'hybrid' foehn wind. *Q J. R. Meteorol. Soc.* **141**, 1857–1869 (2015).

56. Fujibe, F. Urban warming in Japanese cities and its relation to climate change monitoring. *Int J. Climatol.* **31**, 162–173 (2011).

57. Tewari, M., Salamanca, F., Martilli, A., Treinish, L. & Mahalov, A. Impacts of projected urban expansion and global warming on cooling energy demand over a semiarid region. *Atmos. Sci. Lett.* **18**, 419–426 (2017).

58. Bowler, D. E., Buyung-Ali, L., Knight, T. M. & Pullin, A. S. Urban greening to cool towns and cities: a systematic review of the empirical evidence. *Landsc. Urban Plan* **97**, 147–155 (2010).

59. Terada, M., Nagata, T. & Kobayashi, M. "Mobile spatial statistics" supporting development of society and industry—population estimation technology using mobile network statistical data and applications. *NTT Docomo Tech. J.* **14**, 10–15 (2013).

60. Matsubara, N. Grasping dynamic population by "Mobile Spatial Statistics": from the viewpoint of tourism disaster and stranded persons. *J. Info Process. Manag.* **60**, 493–501 (2017).

61. Skamarock, W. C. et al. A description of the Advanced Research WRF version 3. *NCAR Technical Note NCAR/TN–4751STR*, 113. http://www.mmm.ucar.edu/wrf/users/docs/arw_v3.pdf (NCAR, 2008).

62. Kikegawa, Y., Tanaka, A., Ohashi, Y., Ihara, T. & Shigeta, Y. Observed and simulated sensitivities of summertime urban surface air temperatures to anthropogenic heat in downtown areas of two Japanese Major Cities, Tokyo and Osaka. *Theor. Appl. Climatol.* **117**, 175–193 (2014).

63. Kalnay, E. et al. The NCEP/NCAR 40-year reanalysis project. *Bull. Am. Meteorol. Soc.* **77**, 437–472 (1996).

64. Mlawer, E. J., Taubman, S. J., Brown, P. D., Iacono, M. J. & Clough, S. A. Radiative transfer for inhomogeneous atmospheres: RRTM, a validated correlated-k model for the longwave. *J. Geophys. Res. Atmos.* **102**, 16663–16682 (1997).

65. Chou, M.-D. & Suarez, M. J. An efficient thermal infrared radiation parameterization for use in general circulation models. *NASA Technical Memorandum*. 104606, 85 (1994).

66. Matsui, T. et al. Impact of radiation frequency, precipitation radiative forcing, and radiation column aggregation on convection-permitting West African monsoon simulations. *Clim. Dyn.* **55**, 193–213 (2020).

67. Thompson, G., Field, P. R., Rasmussen, R. M. & Hall, W. D. Explicit forecasts of winter precipitation using an improved bulk microphysics scheme. Part II: Implementation of a new snow parameterization. *Mon. Weather Rev.* **136**, 5095–5115 (2008).

68. Mellor, G. L. & Yamada, T. Development of a turbulence closure model for geophysical fluid problems. *Rev. Geophys.* **20**, 851–875 (1982).

69. Janjić, Z. I. The step-mountain eta coordinate model: further developments of the convection, viscous sublayer, and turbulence closure schemes. *Mon. Weather Rev.* **122**, 927–945 (1994).

70. Janjić, Z. Nonsingular implementation of the Mellor-Yamada level 2.5 scheme in the NCEP Meso model. *NCEP Off. Note* **437**, 61 (2002).

71. Chen, F. & Dudhia, J. Coupling an advanced land surface–hydrology model with the Penn State–NCAR MM5 modeling system. Part I: model implementation and sensitivity. *Mon. Weather Rev.* **129**, 569–585 (2001).

72. Kusaka, H. & Kimura, F. Thermal effects of urban canyon structure on the nocturnal heat island: Numerical experiment using a mesoscale model coupled with an urban canopy model. *J. Appl Meteorol. Climatol.* **43**, 1899–1910 (2004).

73. Chen, F. et al. The integrated WRF/urban modelling system: development, evaluation, and applications to urban environmental problems. *Int J. Climatol.* **31**, 273–288 (2011).

74. Ihara, T., Kikegawa, Y., Asahi, K., Genchi, Y. & Kondo, H. Changes in year-round air temperature and annual energy consumption in office building areas by urban heat-island countermeasures and energy-saving measures. *Appl. Energy* **85**, 12–25 (2008).

75. Kikegawa, Y. et al. Validation of a numerical urban weather forecasting model coupled with a building energy model in terms of the reproducibility of solar irradiance and electricity demand. *J. JSCE Ser. G Envir. Res.* **73**, 57–69 (2017).

76. Takane, Y. et al. Future projection of electricity demand and thermal comfort for August in Nagoya city by WRF-CM-BEM. *J. Environ. Engine, AIJ* **80**, 973–983 (2015).

77. Nakajima, K., Takane, Y., Fukuba, S., Yamaguchi, K. & Kikegawa, Y. Urban electricity–temperature relationships in the Tokyo Metropolitan Area. *Energy Build.* **256**, 111729 (2022).

78. Japanese Ministry of Land, Infrastructure, Transport and Tourism. *Nation-wide Road Traffic Condition Study (Road Traffic Census), Fiscal 1999* (2001).

79. Environment Agency of Japan. *The Survey Result on Automobile Exhaust Unit Rate and Total Amounts* (1998).

ACKNOWLEDGEMENTS

AUTHOR CONTRIBUTIONS

Y.T. conceived the study and designed the analyses. Y.T. and K.N. prepared the data for regional climate simulations, and K.N. conducted the simulations and analysis

using the data. Y.T. wrote the original manuscript and K.N. and Y.K. provided comments, feedback and revisions to the manuscript.

COMPETING INTERESTS

The authors declare no competing interests.

ADDITIONAL INFORMATION

Supplementary information The online version contains supplementary material available at https://doi.org/10.1038/s41612-022-00268-0.

Correspondence and requests for materials should be addressed to Yuya Takane.

Reprints and permission information is available at http://www.nature.com/reprints